CHAPTER 3

Plasma diagnostics using probe signals derived from plasma source target

3.1. Introduction

The principal factors influencing the nature of interaction between laser radiation and solid target in vacuum are duration, wave length, power density of the laser pulse and laser light absorption processes as well as physical and chemical properties of the target. The dynamics of the plume produced in laser ablation processes is also of considerable interest in understanding the physics of plasma. Theoretical and experimental investigations are actively in progress in order to obtain accurate knowledge of all the physical processes involved in the ablation processes and the dynamics of laser induced plasma (LIP). Most of the above studies reported are carried out by using conventional Langmuir probes and typical investigation techniques of atomic and molecular physics, such as optical emission and absorption spectroscopy. This chapter deals with information on the LIP generation from metal targets by nanosecond laser metal ablation.

The processes involved in the initial stages of generating plasma from a solid target are complex. It is necessary to consider the heating of the target while in the solid state, the subsequent melting, vaporization and ionization. With high irradiances, ionization can occur very rapidly and since the energy required to ionize an atom is small compared to the energy needed to heat it to temperatures of some millions of degrees. Many theoretical calculations ignore the initial stages of plasma production from a solid target and a cold and fully ionized plasma is assumed to exist with ion and electron densities equal to the solid atom density [1].

The dynamics of plasmas formed from solid targets are governed by the geometry of the target, the laser beam and the time dependence of the laser pulse power and we find it convenient to consider planar targets for our experiment.

3.2. Initial stages of plasma formation from solid targets in vacuum

When laser pulse is incident on an opaque solid target, two extreme situations may be identified. Low irradiances produce only a rise in temperature below the surface, by conduction. If the irradiance is very large, multi-photon ionization takes place at the surface within a few cycles of the electric field and produces phase explosion. Between these extremes, there are a wide variety of intermediate situations governed by changes of phase, pressure due to vaporization, thermionic emission and shockwave generation. Along with this, various thermal, optical and mechanical properties of the target material and their temperature and pressure dependence will also control the interaction.

3.2.1. Light absorption and surface heating

Light (nanosecond duration) falling on the metal target is absorbed by electrons, which are thus raised to higher energy states. These electrons then transfer the energy by collisions with other electrons and phonons so that the solid tends to reach equilibrium at a higher temperature. In order that a single instantaneous temperature may be defined at every point, the light must not cause a substantial change in the internal energy of the region where absorption occurs during the relaxation times involved. The depth at which the temperature reaches a tenth of the surface value is only a few microns even at 50ns [2]. The rate of cooling is rapid, the surface temperature falling to a quarter of the maximum value in in 200ns. Such rapid changes in temperature are accompanied by sudden expansion processes which can generate shock waves in the target [3].

3.2.2. Effects of melting and vapourization

The next stage of heating in the target begins when the temperature is raised to the melting point. However, the transient liquid phase is not of great significance as far as the step towards the production of plasma is concerned. The latent heat of

fusion is small compared with the latent heat of vaporization or the ionization energy. Also, as the laser pulse is of short duration, the molten material will not be displaced significantly during the pulse. But with constant irradiance, the rate of heating increases considerably, together with surface melting. The most important consideration may be change in the optical characteristics of the surface [4].

When the boiling point is reached, effects that are more complex arise. At moderately high irradiances, the rate of evaporation will be greater and the resulting vapour density may become sufficiently large for the bulk of the incident flux to be absorbed in the region occupied by the vapour phase [5]. It should be remembered that the boiling point of a material is pressure-dependent. The radiation pressure due to a focused laser beam can exert a peak pressure of hundreds of atmospheres. When evaporation takes place, the departing particles exert even greater pressure on the surface due to the recoil [6, 7], which affect the physical and chemical properties of the target.

3.2.3. Thermal ionization

The temperature in the hottest region of the vapour generated by the laser pulse will rise as long as the local rate of absorption of energy from the beam is sufficiently large to overcome cooling by expansion and conduction. Eventually, the vapour may reach a sufficiently high temperature for a significant number of atoms to be ionized by collisions. If the vapour is still sufficiently dense, for thermodynamic equilibrium to hold, we may use Saha's equation to relate the densities n_e, n_i, n_a of electrons, ions and neutral atoms at a temperature T:

$$\frac{n_e n_i}{n_a} = \frac{2u_i}{u_a}\left(\frac{2\pi m_e k_B T}{h^2}\right) \exp\frac{-\chi}{k_B T} \qquad (3.1)$$

Here, u_i and u_a are the partition functions for the singly ionized and neutral atoms respectively and χ is the ionization energy of the neutral atom. In the early stages of ionization, only singly ionized atoms are present, so $n_e = n_i$.

At very low electron densities and high neutral atom densities in a lightly ionized vapor, electrons are more likely to absorb photons during free-free transitions, in collision with neutral atoms. The presence of even a small proportion of free electrons causes a marked increase in the absorption coefficient of the

gaseous phase and hence an increase in the rate of heating, leading to a greater degree of ionization. At this stage, free-free transitions of electrons in collision with positive ions become the dominant heating process and thereafter strong absorption occurs. Numerically, the rate of temperature rise is roughly equal to the irradiance [8]. As the temperature rises, the rate of heating increases initially. However as full ionization is approached, the power absorbed per particle begins to fall with increasing temperature and becomes density dependent. At higher densities, three-body recombination becomes the dominant recombination process [9]. In three body recombination, an electron is initially captured by an upper excited level. The electron then cascades down to the ground state either by radiative transitions or by transferring energy to free electrons through collisions.

As the laser fluence increases, the generated plume becomes hotter, resulting in the enhancement of the degree of ionization and thus absorb the incident radiation more efficiently.

3.2.4. Ionization through multi-photon processes

The very high particle densities occurring in solid and in vapour layers generated by intense light will cause strong stark broadening thereby favoring quasi-resonant processes as well as depressing the ionization energy [10]. At very high irradiances, tunneling theory shows that ionization can be extremely rapid and occurs within one or two cycles of electric field. The stimulated Raman effect produced by laser light in a dense medium can produce anti-stokes photons of high frequency [11]. If higher order photons are produced, direct single photon ionization may occur.

3.3. Scope of the work

Target materials get electronically charged, when photo-ablated with an energetically suitable laser pulse. An electrical signal that can be delivered from the target can be used as an alternative probe signal for the diagnostics of LIP.

The ejected species going in to the expanding plume of LIP is responsible for target charging. Laser irradiation in vacuum thus leads to fast rising voltage transients on the target. This may provide information on the nature of ablated species, their expansion velocities and the extent of ionization in the plume. Real

time detection of both electron and ion currents is also possible [12]. Plasma generation and plume evolution processes get reflected on the temporal variations of the time of flight (TOF) spectrum.

The present study deals with the diagnostic aspects of LIP using the signals generated at a copper target. The effects of bias voltage, laser fluence and vacuum level on the plasma dynamics are collected through the signal variations derived from plasma source target.

3.4 Expansion dynamics of laser induced plasma (LIP) in field free space

3.4.1. Experimental works in detail

The plasma is created inside an evacuated chamber (2x10-5 mbar) made of steel. An Nd:YAG laser (Spectra Physics, DCR 11, 10 ns) operating at 10Hz in its fundamental wavelength (1064nm) is used as the laser source for plasma production. A copper disc of 2mm thickness and 20 mm diameter is the target for the focused laser beam. The irradiance is kept at 2.6GW cm^{-2}.

The characterization part involves an active probing technique in the sense that we are not inserting any additional probe into the plasma. It is possible to investigate the history of plasma evolved from the target by looking into the electrical

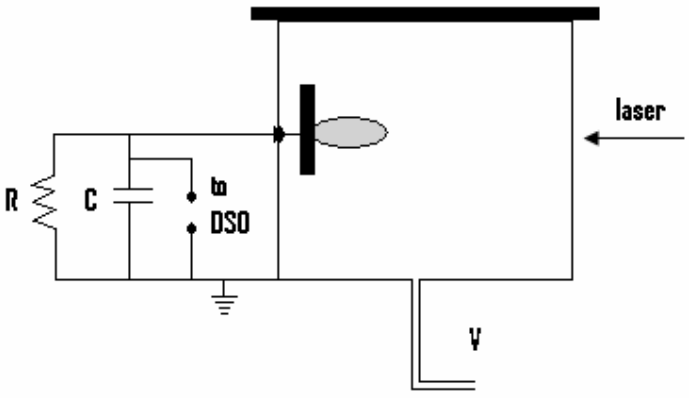

Fig.3.1: Experimental setup to study target signal. V - vacuum pump; R – resistance; C – capacitance; DSO – digital storage oscilloscope.

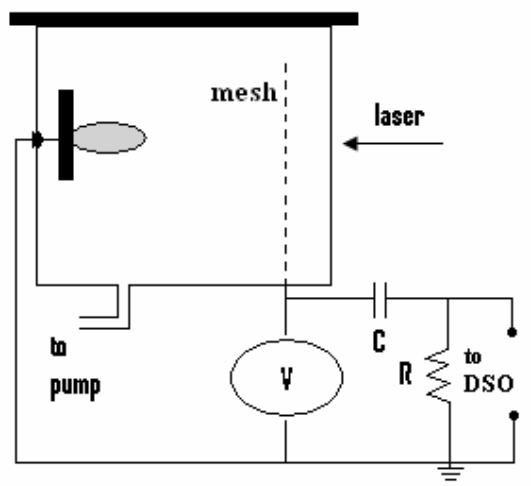

Fig.3.2: Experimental set-up for TOF studies. V- applied bias; C – capacitance; R – resistance; DSO – digital storage oscilloscope.

signal generated at the target itself. The electrical lead taken from the target, for this purpose, is well insulated from the metal chamber. The effects of external parameters on the laser driven plasma can be identified by the temporal variation of voltage transients generated at the target [13]. A schematic diagram of the experimental setup is shown in Fig.3.1. The resistance ($k\Omega$) and capacitance (pF) values are adjusted for the best signal strength.

A TOF spectrum has been recorded with the help of a properly biased mesh, having freedom of translation along the plume expansion direction, erected adjacent to the target. The corresponding experimental setup is given in Fig.3.2. The signal recorded under this arrangement is used for probing the effects of bias voltages, laser fluences and vacuum levels on the plasma dynamics.

3.4.2. Discussion of results

The forward-directed nature of the laser evaporation from planar targets is due to the anisotropic expansion velocities of different species in the plume, imposed by the boundary conditions [14]. The plasma expands freely in vacuum with elliptic contours along the expansion direction which is the target normal.

This is due to the initial density gradient and pressure within the plume, which are much larger in the direction perpendicular to the target surface than in the lateral directions [15]. As the laser pulse triggers the plasma, the peak signal voltage is reached within 80ns.

The transient target charging can be postulated to arise through those electrons which have sufficiently high energies to overcome the plasma work function U and the potential V_T (induced by laser irradiation), escaping from the expanding plasma to the grounded chamber. For a Maxwellian electron energy distribution, it can be shown that the electron current is given by [16, 17]:

$$i_T = i_0 \exp - \left[e(U + V_T) \Big/ kT_e \right] \tag{3.2}$$

where, T_e is the electron temperature and i_0 is a constant. The signal then falls rapidly but sustain for several microseconds. During this time, the behaviour is strongly dependent on the target conditions and the complex processes taking place on the surface layers as well as in the generated plume.

The different peaks superposed on this unipolar pulse correspond to the generation and propagation of species which are at different charged states. Heavier ones take longer times to reach the chamber wall and are delayed more. Fig.3.3 shows the external bias free signal delivered from the target, when irradiated with 200mJ laser energy. This gives an irradiance level, which is well above the plasma generation threshold for copper.

The TOF spectrum of the most prominent species in the plasma has been captured by applying positive and negative polarities to the mesh, arranged adjacent to the target. In both the cases, the ablation produces a bipolar voltage waveform. Calibration of the time-of-flight scale is made by varying the distance between the target and the mesh. The time delay associated with the signal peak can be used to see how their velocities are modified during the transit. A typical TOF profile is given in Fig.3.4.

The ions are accelerated towards the biased mesh and the signal shows a modified time of flight even when the voltage levels are varied. Fig.3.5 shows the

delay in the signal peak when the negatively biased mesh is translated away from the target.

On reversing the polarity (with positive polarity), the electrons are collected by the mesh and an associated negative potential is detected. But it is to be noticed that the voltage waveform is bipolar in nature. During the first 500ns, during which the plasma is highly dynamic, the signal is positive. Thereafter, the signal swings to the negative with a clear twin projection. This can be seen from Fig.3.6. The peak height of the voltage signal is high even when the mesh is negatively biased. In addition to the positive ions collected at the mesh, the secondary electrons generated by neutrals (at the mesh) also may be contributing to this positive voltage.

The velocity distribution of the peak maxima is as shown in Fig.3.7. The appearance of twin peaks is supporting the presence of secondary electrons at the collector.

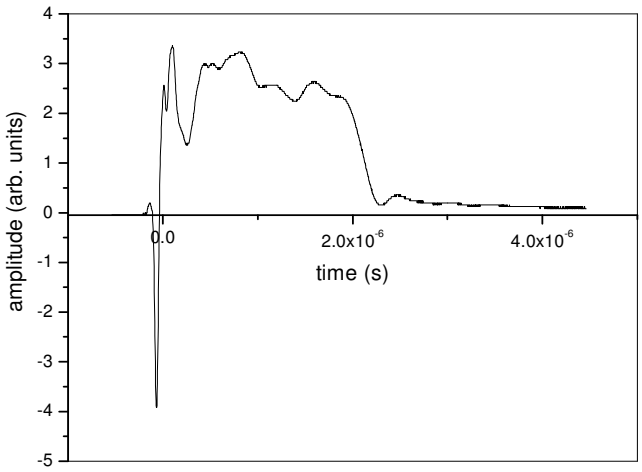

Fig.3.3: Target signal without bias

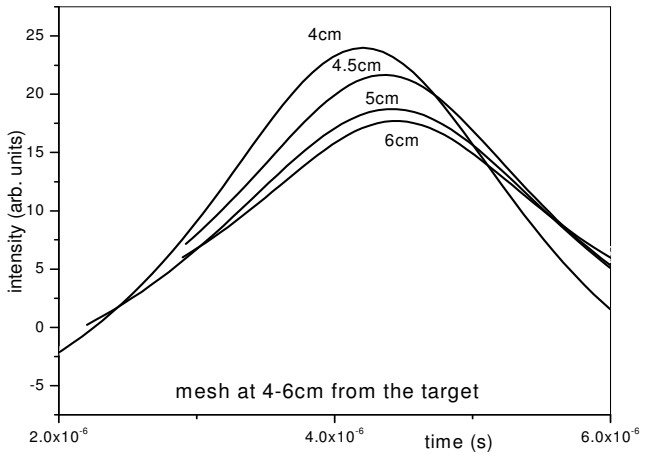

Fig.3.4: A TOF profile of the signal under study, with metallic mesh at various distances from the target.

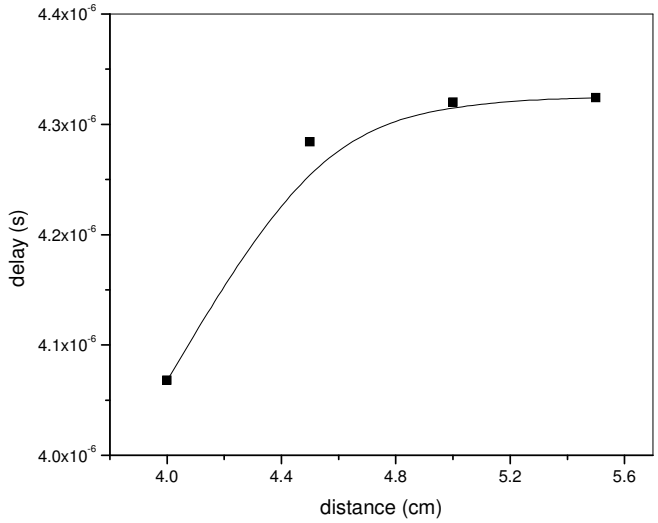

Fig.3.5: Delay in signal peak measured at the negatively biased mesh

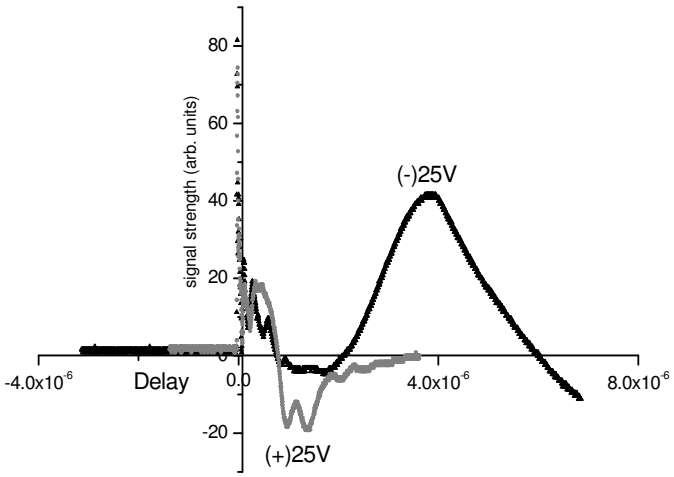

Fig.3.6: Signals with positive and negative bias

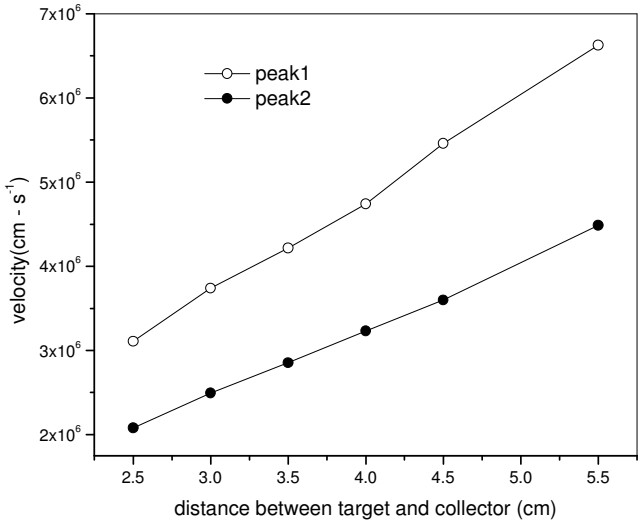

Fig.3.7: Variation of peak velocities with positive bias

The effects of vacuum and power levels on the proposed signal can be seen in Figs.3.8 and 3.9.

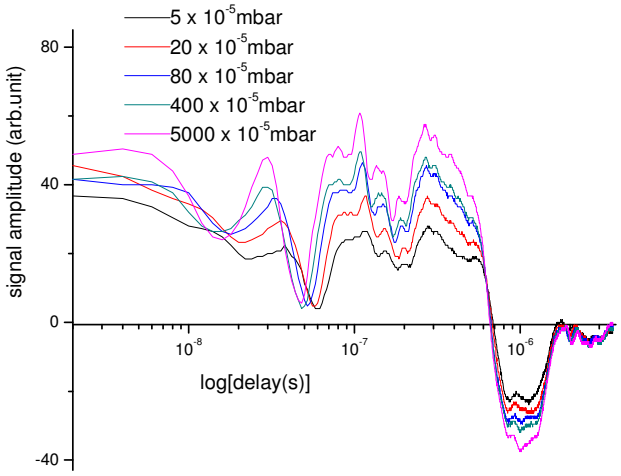

Fig.3.8: signal response to chamber vacuum

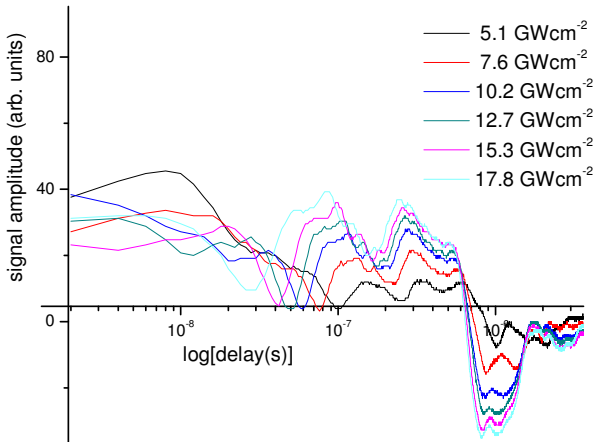

Fig.3.9: Signal response to laser irradiance variation

The responses are collected after applying a fixed moderate positive voltage on the mesh. The chamber pressure is varied from $5x10^{-2}$ mbar to $5x10^{-5}$ mbar of ambient nitrogen. The signal amplitude decreases with increase in vacuum level and as the ambient pressure is decreased, the multiple structure of the profile is clear. This is

probably due to the different species present in the plume gaining more energy in vacuum with an enhancement of secondary electron production. The increase in prominent charge states through collisions with ambient molecules also may be responsible for this effect.

For a given pressure and mesh bias, the signal amplitude and its multiple structure varies also with laser irradiance. Thus, signal response with increase in laser energy shows some analogy with that due to the increase of pressure. The maximum of the distribution is gradually shifted to the left as the energy in increased. This shows the gain in energy of the particles in the distribution.

3.4.3. Summary

Different charged states of the same atom can be tracked from the signal [18]. The signal shows a double peak distribution with positive polarity and a modified time of flight when the voltage levels are varied. As the ambient pressure is decreased, the multiple structure of the peak becomes clear. It seems that the method, when implemented together with suitably designed Langmuir probes can throw more light on the hidden aspects of this technique.

3.5. Effect of external magnetic field on the probe signals

Effects of parameters like external magnetic field on LIP can also be studied by the response of the corresponding electrical signal from the plasma source target.

3.5.1. Introduction

The use of a magnetic field with laser-created plasma is especially interesting, as the magnetic field can be used to control the properties of the transient and dynamic plasma state. The collimation and stability properties of plasma flow across a magnetic field are of particular relevance to the propagation of charged particle beams, stellar bipolar flows, solar wind evolution etc. In inertial fusion, confinement of expanding plasma using a magnetic field offers a potential means to slow high energy particles before they implant in surrounding structures [19, 20]. Spectroscopic studies of dynamics of the plume species in the presence of a magnetic field showed that their spatial and temporal characteristics change considerably with their charge state.

The presence of a magnetic field during the expansion of laser produced plasma may initiate several interesting physical phenomena including conversion of plasma thermal energy into kinetic energy, plume confinement, ion acceleration, emission enhancement, plasma instabilities etc. [21]. It has been postulated that a cloud of laser produced plasma will be stopped by a magnetic field B within a distance $R \sim B^{-2/3}$. Apart from its basic research importance, the effect of a

magnetic field on the expansion dynamics of LIP plumes also has importance in applied research. The effectiveness of debris reduction using magnetically guided pulsed laser deposition has been demonstrated by previous workers [22, 23].

3.5.2. Experiment and results

The effects of external magnetic field on the laser driven plasma can be identified by the temporal variation of voltage transients generated at the target. A schematic diagram of the experimental setup is shown in figure 3.10. The circuit is closed by the emitted charged species travelling towards the chamber wall at velocities greater than $2x10^6$ cm/s [13, 18]. As the laser pulse triggers the plasma, the signal rises to positive within 5ns. This is due to the creation of plasma on the target surface and is unaffected by the application of external magnetic field. This signal showing some characteristic variations as the plume expands is always positive until it finally drops to zero, after two microseconds.

Magnetic field is applied on LIP in a direction transverse to plasma expansion. Two disc shaped magnetic pole pieces (4cm diameter) are used to apply a magnetic field of maximum flux density 0.2T. The magnets placed inside suitable non-magnetic housings are given required separations to change the field in-between. The target is carefully aligned outside the field so that the generated plume expands into the field. Absolute calibration of the field strength has not been performed. For qualitative analysis, the separation between the pole pieces is varied. The results of field mapping have shown that the field is inhomogeneous when the pole pieces are closer (< 4.5 cm). As the pole pieces are separated, the field becomes more and more homogeneous (7.5cm > separation between the poles > 4.5cm). Thereafter, an inhomogeneous decrease in field strength is observed (separation between the poles > 7.5cm) and at each instance, the plasma responds to the field variations as observed in Fig.3.11.

On applying the magnetic field, the trajectories of different charged particles in the plasma and their kinetic energies are modified and they enter into newly defined territories. The plasma confinement (though small) induced by the field should increase the collision frequency of the charged species by confining them to smaller volumes. The plume front decelerates in the direction normal to the target surface and the ion density in the plasma rises immediately. At this point of time, the possible recombinations and their rates get modified and the target experiences a deficiency of positive charge which pulls the signal negative. At later times, the plume tries to

expand in the direction of the magnetic field and the signal grows more and more positive. It is noted that, the transition to positive signal is delayed in intense fields.

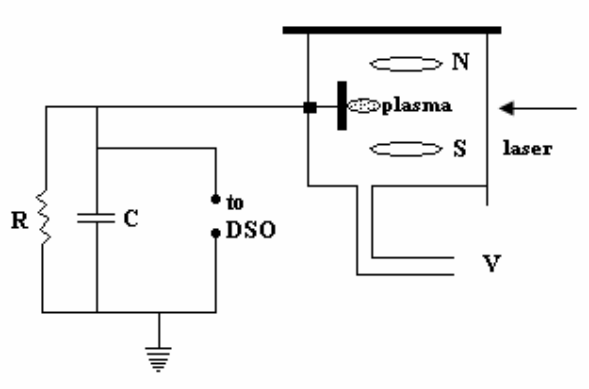

Fig.3.10: schematic diagram of the experimental set-up. [N-North pole, S-South pole, V-vacuum pump, R–resistance, C-capacitance and DSO-digital storage oscilloscope.

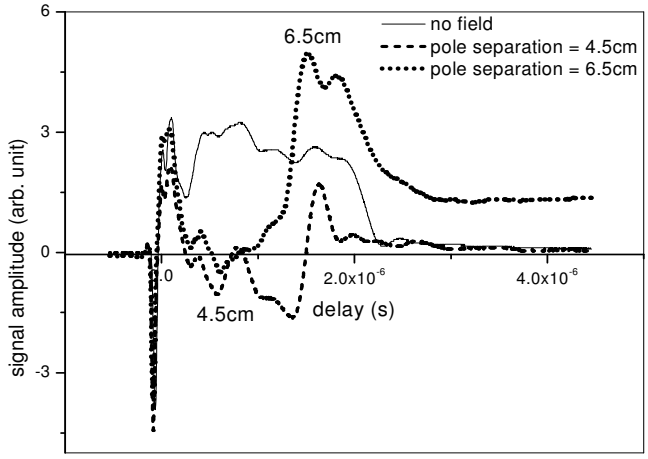

Fig.3.11: Effect of magnetic field on the signal. Two different field strengths are applied. [Absolute calibration of the field strength has not been performed. For qualitative analysis, the separation between the pole pieces are varied.]

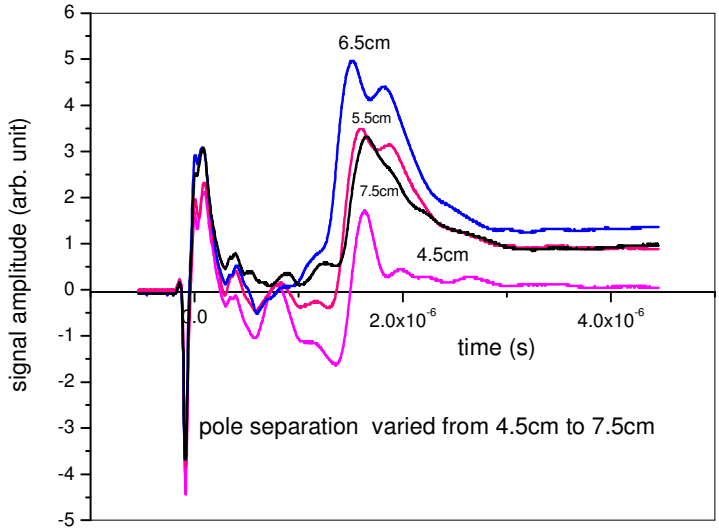

Fig.3.12: Signals showing the effects of magnetic field on the dynamics of plasma. [Absolute calibration of the field strength has not been performed. For qualitative analysis, the separation between the pole pieces are varied.]

Figure 3.12 shows the signal extracted from the target when the magnetic field intensity is systematically varied. The strong signals around 1.5μs and 1.85μs are especially noticeable. Both are delayed in a homogeneous field. In the no field case, the signal falls to zero at 2.3μs after the laser pulse. In the presence of field, the signal exists for longer time. This shows that the plume lifetime is increased in the presence of magnetic field.

3.5.3. Summary

The plasma expansion dynamics in magnetic field has been investigated by monitoring the voltage transients generated at the target. The signal in the presence and absence of magnetic field is analyzed to investigate on the plasma responses to the field. The field confines the plasma and the charged particles enter into new territories, with modified trajectories and kinetics. Signs of a transverse expansion are evident. An increased plume lifetime is observed in the presence of the field.

3.6. References

[1] T. P. Hughes, Plasmas and laser light (Adam Hilger, London, 1975)

[2] Ready J. F., J. Appl. Phys. 36 462 (1965)

[3] Steverding B., J Phys D 3 358 (1970)

[4] Bonch Bruevich, A M Imas Ya A, Romanov G S, Libenson M N, Maltsev L N, Sov. Phys. Tech. Phys. 13 640 (1968)

[5] Anisimov S. I., Bonch-Bruevich A M, El Yashevich M A, Imas Ya A, Pavlenko N A, Romanov G. S., Sov. Phys. Tech. Phys. 11 945 (1967)

[6] Askaryan G. A. and Moroz E M, Sov. Phys JETP 16 1638 (1962)

[7] Hughes T P, Proceedings of conference on lasers and their applications, (sponsored by IEEE and Science divisions, London), pp. 5-12 (1964)

[8] Archbold E., Harper D W, Hughes T P, J Appl Phys 15 1321 (1964)

[9] Martineau J and Tonon G, Phys Lett. 30A, 32 (1969)

[10] Farkas Gy. Horvath Z. Gy., Kertesz I, Phys Lett 39A 231 (1972)

[11] Mennincke H, Phys Lett 37A 381 (1971)

[12] S. H. Brongersma, J. C. S. Kools, T. S. Baller, H. C. W. Beijerinck and J. Dieleman, Appl. Phys. Lett. Vol. 59 No.11 1311 (1991)

[13] P. E. Dyer, Appl. Phys. Lett. Vol 55, No.16 1630 (1989)

[14] Rajiv K. Singh and J. Narayan, Phys. Rev. B 41 8843 (1990)

[15] S. S. Harilal, M. S. Tillack, B. O'Shay, C. V. Bindhu and F. Najmabadi, Phys. Rev E, Vol 69 26413 (2004)

[16] Robert F. Benjamin, Gene H. McCall and A. Wayne Ehler, Phys. Rev. Lett. 42 890 (1979)

[17] G. Cook and P E Dyer, J. Phys. D 16 889 (1983)

[18] R. J. Von Gutfeld and R W Dreyfus, Appl. Phys. Lett. 54 (13) 1212 (1989)

[19] W. Gekelman, M. Van Zeeland, S. Vincena and P. Pribyl, J. Geophys. Res.[Space Phys.] Vol 108 1281(2003)

[20] H. C. Pant, Phys. Scr. Vol T 50 109 (1994)

[21] D. K. Bhadra, Phys. Fluids Vol 11 234 (1968)

[22] R. Jordan, D. Cole and J. G. Lunney, Appl. Surf. Sci. Vol 110 403(1997)

[23] Y. Y. Tsui, H. Minami, D. Vick and R. Fedosejevs, J. Vac. Sci. Technol. Vol A 20 744 (2002)